Drug Design, Development and Therapy

Dovepress
Taylor & Francis Group

Open Access Full Text Article

ORIGINAL RESEARCH

Study of the Chemical Composition and Anti-Inflammatory Mechanism of Shiyiwei Golden Pill Based on UPLC-Q-TOF/MS and Network Pharmacology

Cong Han[1,*], Jing Chen[2,*], Chuanlin Shen[1], Qiuxia Liang[1], Ying An[1], Chaoyi Zhou[1], Kechun Liu[1], Qing Xia[1], Qiuxia He[1], Huazheng Zhang[3]

[1]Biology Institute, Qilu University of Technology (Shandong Academy of Sciences), Jinan, Shandong, People's Republic of China; [2]Department of Tibetan Medicine, Tibetan Traditional Medicine College, Lhasa, Tibet, People's Republic of China; [3]Shandong Academy of Chinese Medicine, Jinan, Shandong, People's Republic of China

*These authors contributed equally to this work

Correspondence: Qing Xia, Biology Institute, Qilu University of Technology (Shandong Academy of Sciences), Jinan, 250103, People's Republic of China, Email sdxq1021@163.com; Huazheng Zhang, Shandong Academy of Chinese Medicine, Jinan, 250014, People's Republic of China, Email zhanghuazheng1109@163.com

Purpose: Shiyiwei Golden Pill (SYW) is a classic traditional prescription used to treat mKhris-pa according to the theory of Tibetan medicine. At present, SYW is widely used to treat cholecystitis in Tibetan areas. However, the chemical constituents and anti-inflammatory mechanisms are still largely undiscovered. This study aimed to investigate the chemical composition and anti-inflammatory effects of SYW, as well as its potential mechanisms.

Methods: The components of SYW were identified using ultrahigh-performance liquid chromatography with quadrupole time-of-flight mass spectrometry (UPLC-Q-TOF/MS). The anti-inflammatory effects of SYW were determined on zebrafish and RAW264.7 cell inflammation models. Additionally, we predicted the targets and pathways of SYW to confirm its anti-inflammatory effects using network pharmacology approaches. Finally, a quantitative real-time polymerase chain reaction (qRT–PCR) was performed to validate the expression of genes associated with anti-inflammatory pathways.

Results: We identified 94 compounds in SYW, mainly alkaloids, phenols, and flavonoids. SYW inhibited inflammatory cell proliferation and migration in the three zebrafish inflammation models. In the RAW264.7 cell model, SYW suppressed the levels of NO and pro-inflammatory cytokines. In addition, network pharmacology analysis revealed that ALB, IL6, TNF, AKT1, and EGFR were identified as the potential key targets of SYW. KEGG enrichment and qRT–PCR analysis showed that PI3K/Akt/FoxO signaling pathway was involved in the anti-inflammatory effects of SYW.

Conclusion: Herein, we identified 94 chemical constituents of SYW and demonstrated that SYW exerts anti-inflammatory effects by regulating the PI3K/Akt/FoxO signaling pathway.

Keywords: shiyiwei golden pill, inflammation, zebrafish, network pharmacology, PI3K/Akt/FoxO signaling pathway, cholecystitis

Introduction

Cholecystitis, characterized by inflammation of the gallbladder, is usually caused by cholestasis due to bile duct blockage, and is always accompanied by gallbladder infection. According to epidemiological surveys, the prevalence of chronic cholecystitis in Chinese adults is 1.42% to 7.06%, and the prevalence also increases with age.[1,2] Studies have shown that suppression the production of pro-inflammatory cytokines can ameliorate cholecystitis.[3] Taking antibiotics and surgery are the most common treatment strategy of cholecystitis in the clinic. The theory of traditional Tibetan medicine (TTM) has a unique understanding of cholecystitis, which believes cholecystitis belongs to the category of

Received: 25 November 2024
Accepted: 10 April 2025
Published: 24 April 2025

mKhris-pa. MKhris-pa refers to an essence that does not vanish but rather descends from the liver to the gallbladder.[4] The qualities of mKhris-pa are associated with inflammation.[5] According to this theory, diet and daily living therapy, drug therapy and other treatment methods have been proposed, and have achieved remarkable curative effects in clinical treatment of cholecystitis.[6]

Shiyiwei Golden Pill (SYW), a classic TMM formula, is used to treat the mKhris-pa. It is composed of eleven kinds of Tibetan medicinal materials, including *Terminalia chebula Retz*. (Hezi), dry faeces of *Sus scrofa L*. (Heibingpian), *Punica granatum L*. (shiliuzi), brag-zhun (Zhaxun), *Herpetospermum caudigerum Wall*. (Bolengguazi), *Aconitum tanguticum(Maxim).Stapf*. (Tanggutewutou), *Hypecoum erectum L*. (Jiaohuixiang), *Embelia oblongifolia Hemsl*. (Suantengguo), *Rosa multiflora Thunb*. (Qiangweihua), *Aconitum pendulum Busch* (Tiebangchui), and artificial musk (Rengong Shexiang). At present, SYW has become a clinically essential drug for treating cholecystitis and hepatitis in the Tibetan areas of China. Previous studies have manifested that SYW combined with antibiotics can improve the clinical cure rate and treatment efficiency of chronic cholecystitis.[7] However, the current research on SYW mainly focuses on prescription compatibility, its chemical composition and the anti-inflammatory mechanism of SYW remain largely unrevealed, which awfully hinders the clinical promotion and rational use of SYW. Although few articles reported the modern research of SYW, some of the SYW formula medicines have been covered to have anti-inflammatory effects. For instance, *Terminalia chebula Retz* extract inhibited inflammation in cells and rats by regulating inflammasome signaling.[8,9] Pomegranate seed oil (Seed oil of *Punica granatum L),* has anti-inflammatory effects that may be effective in inhibiting TNF-α and inflammatory diseases.[10] The ethyl acetate extract of Semen Herpetospermi (*Herpetospermum caudigerum Wall),* alleviated cholestasis by reducing inflammation.[11] The petroleum ether fraction and ethanol extract of *Rosa multiflora Thunb,* hips showed an anti-inflammatory effect.[12,13]

As we know, the chemical composition of prescriptions serves as the material basis for the effect.[14] The components of Tibetan medicines are highly complex. At present, there are some scientific and reliable methods to infer its drug-effect relationships, such as UPLC-Q-TOF/MS and zebrafish. UPLC-Q-TOF/MS has been successfully used to analyze compounds in TTM prescriptions, which has the advantages of high resolution and high speed.[15] Zebrafish has been widely used in anti-inflammatory activity evaluation due to its several advantages, such as body transparency, sharing similar inflammatory mediators and receptors with humans, high throughput, and so on.[16] Interestingly, in *Tg (lyz: EGFP)* transgenic zebrafish, the neutrophils are fluorescently labeled, making the neutrophils easily real-time visualized in vivo under a fluorescence microscope. Network pharmacology can systematically clarify the intricate biological interactions among medicines, targets, and diseases, provide a promising method to predict the chemical basis and mechanism of TMM. In recent years, network pharmacology has been used to investigate the mechanism of Tibetan medicine such as Dida and Si-Wei-Qiang-Wei in treating Cholecystitis.[3,17] However, the action mode of TMM is quite complex, and the results of network pharmacology require justification by experiments. Characterized by its excellent reproducibility and broad quantitative range, qRT–PCR is a benchmark for quantifying gene expression.[18] This method is increasingly employed to validate network pharmacology results.[19]

Currently, we first analyzed the chemical composition of SYW by UPLC-Q-TOF/MS. Subsequently, the anti-inflammatory effects of SYW were evaluated in three distinct zebrafish inflammation models and a cell inflammation model induced by lipopolysaccharide (LPS). The anti-cholecystitis mechanism of SYW was evaluated by a combination of network pharmacological analysis and quantitative real-time polymerase chain reaction (qRT–PCR) verification. So as to provide an experimental foundation for the further development and utilization of SYW in treating cholecystitis.

Materials and Methods

Chemicals

LPS was purchased from Sigma-Aldrich (St. Louis, MO, USA). $CuSO_4$•$5H_2O$ was purchased from Sinopharm Chemical Reagent Co., Ltd (Shanghai, China). Cell counting kit-8 (CCK-8) was obtained from Dingguo Changsheng Biotechnology (Beijing, China). The tumor necrosis factor-α (TNF-α), interleukin-1β (IL-1β), and interleukin-6 (IL-6) ELISA kits were acquired from ABclonal Biotechnology (Hubei, China). The total nitric oxide assay kit was purchased from Beyotime (Jiangsu, China).

Preparation of the SYW Sample Solution

The Ultrasound-Assisted Extraction was used to prepare the SYW sample solution.[20] We first weighed 2 g of the SYW sample and added 20 mL of 50% methanol to ultrasonically extract three times, with the ultrasonic power set at 300 W and the ultrasonic extraction time set at 1 h. After filtering, the supernatant was combined and decompressing concentrated using a rotary evaporator at 50 °C. Following this, the precipitate was freeze-dried by vacuum. The extraction rate was 38.16%.

UPLC-Q-TOF/MS Analysis Chemical Constituents of SYW

Waters H-Class HPLC system (Waters Corporation, Milford, MA, USA) and AB Sciex Triple TOF® 4600 mass spectrometer (SCIEX Company, MA, USA) were utilized to analyze the chemical constituents of SYW. The analytical column, an Agilent ZORBAX RRHD Eclipse XDB-C18 (2.1×100 mm, 1.8 μm) was operated at 30 °C. The mobile phase comprised of solvent A (acetonitrile) and solvent B (0.1% formic acid in water). Chemical constituents were separated with the following gradient: 0–3 min, 95%B; 3–20 min, 95%-70%B; 20–35 min, 70%-10%B; 35–38 min, 10%B; 38–38.1 min, 10–95%B; 38.1–40 min, 95%B. The constant injection volume was maintained at 2 μL, while the flow rate was consistently established at 0.3 mL/min.

Positive and negative ion scanning mode, and an electrospray ionization (ESI) source was utilized. The mass parameters were listed as follows: ion source gas 1: 50 psi, ion source gas 2: 50 psi, curtain gas 35 psi, ion spray voltage floating of 550 or −4500, ion source temperature of 500 °C, mass range obtained was from m/z 50 to 1250. Compounds were identified based on the high-resolution mass spectrometry database and pertinent literature.

Anti-Inflammatory Activity of SYW in Zebrafish

Zebrafish Breeding

Tg (lyz: EGFP) transgenic zebrafish were obtained from Shandong Academy of Sciences. Healthy mature zebrafish were placed in spawning tanks, and the male-to-female ratio was 2:2. After that, zebrafish embryos were collected between 12:00 and 14:00 on the following day. Then, the zebrafish embryos were put into zebrafish culture water, and 0.1% methylene blue solution was added. In addition, the zebrafish embryos were cultured at 28 ± 0.5 °C (light 14 h, dark 10 h). We adhered to the standard ethical guidelines for all the experiments from the Shandong Academy of Sciences and the ethics approval reference number was SWS20230427.

Anti-Inflammation Effect of SYW on $CuSO_4$-Induced Zebrafish Model

Zebrafish larvae, precisely at three days post-fertilization (dpf), were chosen and transferred to 24-well plates (n = 8 larvae / 8 wells per group). The experiment involved five groups: a control group, a model group, and SYW treatment groups (25, 50, and 100 μg/mL). The control and model groups continued to be incubated with zebrafish culture water, the SYW-treated groups were treated with different concentrations of SYW. $CuSO_4$ (40 μM) was applied to the model and SYW-treated groups following a 24 h incubation period. After 1 h, a SZX16 fluorescence microscope (Olympus, Tokyo, Japan) was utilized to visualize the location of inflammatory cells in the zebrafish. Additionally, we tallied the quantity of inflammatory cells that moved toward the lateral line.

Anti-Inflammation Effect of SYW on Tail-Cutting Zebrafish Model

Zebrafish larvae at 3 dpf were randomly placed in 24-well plates (n = 6 larvae / 6 wells per group) and divided into control, model, and SYW treatment groups (25, 50, and 100 μg/mL). Except for those in the control group, zebrafish tails were amputated using a blade at the same location. The control and model groups were subsequently placed in zebrafish culture water. The SYW-treated groups were treated with different concentrations of SYW. Each group was incubated at 28 °C for 6 h. After 6 h, the fluorescence microscope was used to observe the inflammatory cells in the damaged area.

Anti-Inflammation Effect of SYW on LPS-Induced Zebrafish Model

Zebrafish larvae at 3 dpf were randomly placed in 24-well plates (n = 10 larvae / 10 wells per group). The experiment involved control, model, and SYW treatment groups (25, 50, and 100 μg/mL). Every group received different treatments. To treat the control group, zebrafish culture water was used. The model group was treated by LPS (100 μg/mL). The

SYW treatment received different concentrations of SYW and LPS concurrently. After 3 days, the fluorescence microscope was utilized to observe the inflammatory cells.

Anti-Inflammatory Activity of SYW in vitro

Cell Culture

RAW264.7 cells were obtained from Wuhan Pricella Biotechnology Co., Ltd (Hubei, China). RAW264.7 cells were cultured in a high-glucose medium, which was supplemented with 10% fetal bovine serum and 1% penicillin-streptomycin solution at 37 °C with 5% CO_2.

The Effects of SYW on Cell Viability

RAW264.7 cells were preincubated for 24 h in 96-well plates (1.5×10^4 cells/well). The cells were exposed to different concentrations of SYW (1.25, 2.5, 5, 10, 25, and 50 μg/mL). After 24 h, we added CCK-8 reagent (10%) to each well. After 30 minutes, the absorbance was measured by a microplate reader.

The Impact of SYW on Nitric Oxide Generation

The concentration of nitric oxide was determined using a NO detection kit. Concisely, RAW264.7 cells were treated with 1.25, 2.5, 5, and 10 μg/mL of SYW for 3 h, then the model group and SYW group were mixed with LPS (1 μg/mL) for 24 h. According to kit instructions, we took the cell supernatant to measure nitric oxide production via the microplate reader. The concentration was calculated by comparing the absorbance and the standard curve.

The Impact of SYW on IL-1β, IL-6, and TNF-α Release in Cells

The concentrations of IL-1β, IL-6, and TNF-α were obtained by using ELISA kits. In short, the SYW treatment groups were cultured with various concentrations of SYW (1.25, 2.5, 5, and 10 μg/mL). Other groups were treated with a cell culture medium. After incubating for 3 h, LPS (1 μg/mL) was added to the model and SYW groups for 24 h. According to the kit instructions, we collected the cell supernatant to measure the levels of IL-1β, IL-6, and TNF-α.

Network Pharmacology

Target Prediction of SYW

The components with a relative content greater than 1% were considered as the main components of SYW and selected for the subsequent analysis. The PubChem database (https://pubchem.ncbi.nlm.nih.gov/) was utilized to get typical SMILES or two-dimensional structures of these components. Thereafter, possible active targets of each component of SYW were retrieved from the PharmMapper (http://www.lilab-ecust.cn/pharmmapper/) and Swiss Target Prediction databases (http://swisstargetprediction.ch/). The names of the genes were corrected by using the UniProt database (https://www.uniprot.org/) after removing duplicates.

Cholecystitis-Related Targets Prediction

The targets of cholecystitis were found in DisGeNET (https://disgenet.com/) and GeneCards databases (https://www.genecards.org/). After removing duplicates, cholecystitis-related targets were collected.

Construction of the SYW-Target-Cholecystitis Network

The Venn database (http://bioinformatics.psb.ugent.be/webtools/Venn/) was utilized to obtain the intersection targets between cholecystitis and SYW. Then, these data were used to make a SYW-Target-Cholecystitis to visually examine the network.

Topological Analysis

The targets of SYW components playing anti-cholecystitis roles were loaded into the String platform (https://string-db.org/). The species was set as "Homo sapiens", and the minimum interaction threshold was set to "high confidence" (> 0.7). Subsequently, the protein-protein interaction (PPI) network was created to analyze the key target where SYW exerts its anti-cholecystitis effects. In addition, Centiscape 2.2 was used to analyze and calculate the degree centrality (DC), closeness

centrality (CC), and betweenness centrality (BC). The targets with DC, BC, and CC values exceeding the median were retained to construct the core target network of SYW and cholecystitis.

Analysis of GO and KEGG Enrichment

Gene ontology (GO) and Kyoto encyclopedia of genes and genomes (KEGG) enrichment analyses were performed on the DAVID database (https://david.ncifcrf.gov/). The top 20 of GO and KEGG terms were selected to be plotted.

Detection of Gene Expression Levels in Zebrafish

Zebrafish larvae at 3 dpf were divided into control, model, and SYW treatment groups (25, 50, and 100 μg/mL). The SYW-treated groups were treated with different concentrations of SYW for 24 h. After that, $CuSO_4$ (40 μM) was applied to the model and SYW-treated groups for 1 h. At the conclusion of the experiments, twenty larvae were pooled as a single replicate, with three replicate wells utilized for each experimental group. The total RNA was extracted using FastPure Cell/Tissue Total RNA Isolation Kit V2. Additionally, to transcribe the RNA into cDNA, HiScript III RT SuperMix was utilized. Then, qRT–PCR was conducted with a SYBR Green fluorescence quantitative PCR kit. The $2^{-\Delta\Delta Ct}$ method was utilized to determine gene expression, and *rpl13a* was chosen as the reference gene.[21] Table 1 shows the primer sequences.

Statistical Analysis

Foremost, the data is analyzed by normality and lognormality tests. Then, it was subjected to a one-way analysis of variance (ANOVA). A difference was deemed statistically significant when $P < 0.05$. All data are presented as mean ± standard error of the mean (SEM).

Table 1 Primer Sequences

Gene	Forward Primer	Reverse Primer
akt1	5′-GTTGGTTCCTCCGTTCAAGC-3′	5′-GGTCGTCTCTCGCTGTCAAA-3′
bcl6	5′-ACCCGCTAACCTCAAAACCC-3′	5′-CAGAACATGAGCCCGAAGGT-3′
egfr1	5′-TTCTTTCACCCGCACTCCTC-3′	5′-CCGCCAGAGAAAACTGACCA-3′
esr1	5′-TATGACCTGTTGCTGGAGATG-3′	5′-CGCCGTTGGACTGAATGG-3′
foxo1	5′-TGGACCTACCCACAGTCACA-3′	5′-GACCTGAGCCTCCATACTGC-3′
hras	5′-CTCAGCCAAAACCAGGCAAG-3′	5′-TCGTCTGGTGGATTCAGCTTC-3′
il1β	5′-CATTTGCAGGCCGTCACA-3′	5′-GGACATGCTGAAGCGCACTT-3′
il6	5′-TCAGCACTCCTCTCCTCAAA-3′	5′-ATCCATCTCTCCGTCTCTCAC-3′
il7ra	5′-TGAAAAGCCATCTGCCCCTG-3′	5′-CTCTCTCGGAAGCCGTTCAT-3′
irs1	5′-TAGGCTGACACGTCCAACAC-3′	5′-AAACAGGTGGGAACAGCGAT-3′
mapk3	5′-TTTGARCACCAGACCTACTGCCAG-3′	5′-TAGCAGATATGGTCRTTGCTGAG-3′
mmp9	5′-TGCCAACGAAACCTTCTCCA-3′	5′-CCTTGATTTGGCAGGCATCG-3′
pik3ca	5′-GCACGAGACCATGCAATGAC-3′	5′-ACAATACTGCCTGTGCCTCC-3′
ptgs2	5′-TATTACACCCGCACCCTTGC-3′	5′-GTGAGAGAAATGCTGGGCGA-3′
rpl13a	5′-CGGTCGTCTTTCCGCTATTG-3′	5′-CTTGCGGAGGAAAGCCAAAT-3′
tnf-α	5′-GGAGAGTTGCCTTTACCGCT-3′	5′-CCTGGGTCTTATGGAGCGTG-3′
vegf	5′-TGTGACCGTCTACCATAT-3′	5′-ATTAAGGCTCTCCATTCG-3′

Results

Chemical Constituent Analysis of SYW

As exhibited in Figure 1, a total of 94 compounds were identified in SYW, including 22 kinds of alkaloids, 28 kinds of phenols, 11 kinds of flavonoids, 7 kinds of terpenoids, 6 kinds of tannins, and 20 other compounds. Then the relative content of each compound was calculated from the peak area. Among them, 28 components had a relative content greater than 1%, such as gallic acid, 3-galloylshikimic acid, and 1.6-di-O-galloyl-β-D-glucose. These 28 compounds are labeled with asterisks in Table 2.

Anti-Inflammatory Activity of SYW in Zebrafish

SYW Alleviates $CuSO_4$-Induced Inflammation

$CuSO_4$ can activate inflammatory responses in zebrafish, which is characterized as the migration of inflammatory cells to the lateral line. As shown in Figure 2A, the number of fluorescent cells in the model group was considerably increased at the lateral line compared to that in the control group. Nonetheless, the SYW treatment (25, 50, and 100 μg/mL) considerably decreased the neutrophil counts in a dose-dependent manner compared to that in the model group ($P < 0.01$) (Figure 2D). This indicated that the SYW treatment could alleviate the inflammation induced by $CuSO_4$ in zebrafish.

SYW Alleviates Tail-Cutting-Induced Inflammation

The migration of inflammatory cells to the zebrafish tail indicated that an inflammatory response occurred at the wound. As shown in Figures 2B and E, the inflammatory cells in tail-cutting zebrafish accumulated at the wound area (red box area) than that in the control group ($P < 0.01$). The SYW reduced the aggregation of inflammatory cells in a dose-dependent manner ($P < 0.01$), indicating that SYW could suppress tail-cutting-induced inflammation.

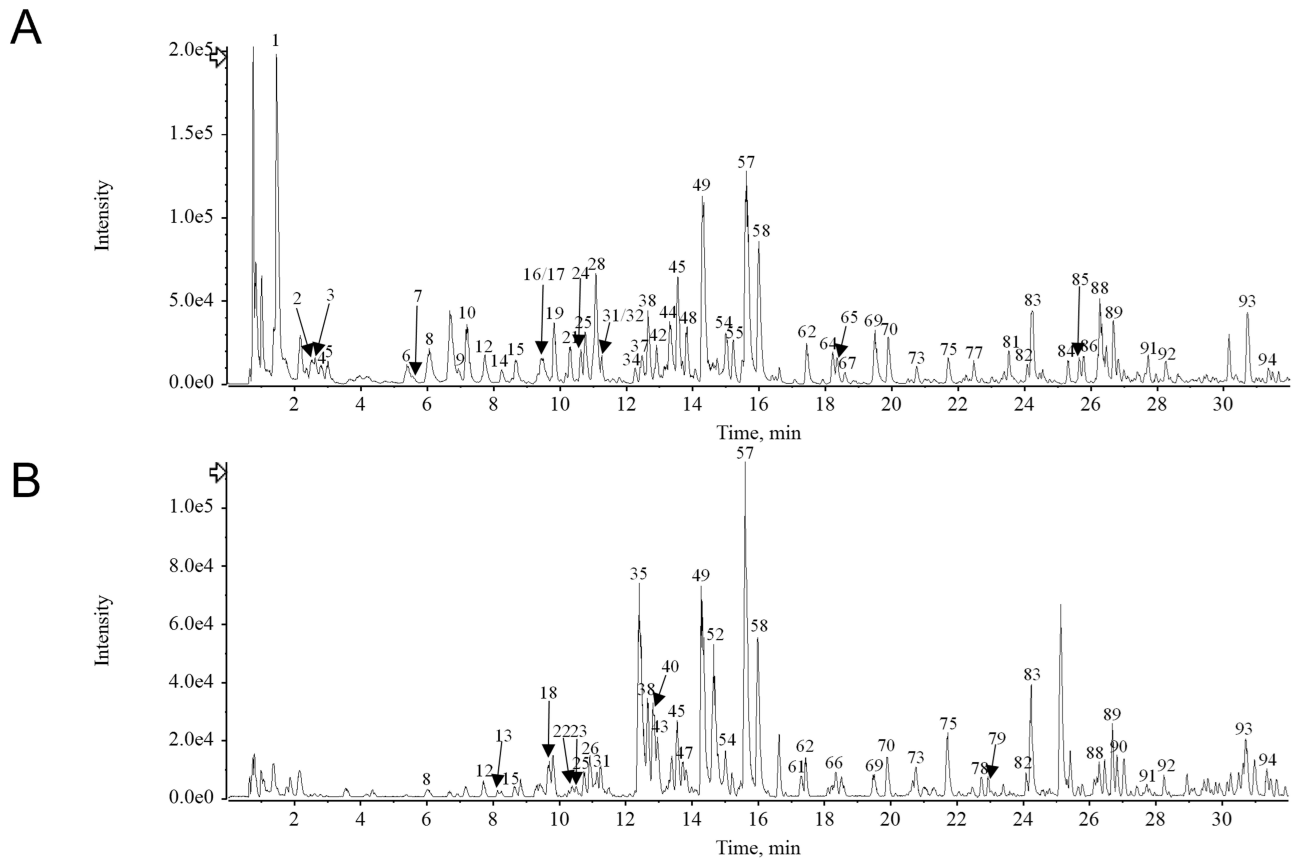

Figure 1 Total ion chromatogram of UPLC-Q-TOF/MS analysis. (**A**) Base Peak Chromatogram (BPC) of SYW samples in ESI- mode. (**B**) BPC of SYW samples in ESI+ mode.

Table 2 Identification Results of Main Components of SYW Samples

Number	Name	Molecular Formula	Molecular Weight	Retention Time (min)	Comparative Content (%)
1*	Gallic acid	$C_7H_6O_5$	170.02	1.46	6.87%
2*	3-Galloylshikimic acid	$C_{14}H_{14}O_9$	326.06	2.53	1.33%
3	4-Galloylshikimic acid	$C_{14}H_{14}O_9$	326.06	2.62	0.07%
4	5-Galloylshikimic acid	$C_{14}H_{14}O_9$	326.06	2.81	0.73%
5	Hydroxytyrosol 1-O-glucoside	$C_{14}H_{20}O_8$	316.12	2.94	0.71%
6	Methyl gallate 3-O-β-D-glucoside	$C_{14}H_{18}O_{10}$	346.09	5.41	0.77%
7	1,4-di-O-Galloyl-β-D-glucose	$C_{20}H_{20}O_{14}$	484.09	5.66	0.45%
8*	1,6-di-O-Galloyl-β-D-glucose	$C_{20}H_{20}O_{14}$	484.09	6.07	1.77%
9	3,6-di-O-Galloyl-β-D-glucose	$C_{20}H_{20}O_{14}$	484.09	6.95	0.48%
10*	1,3-di-O-Galloyl-β-D-glucose	$C_{20}H_{20}O_{14}$	484.09	7.21	2.05%
11	Heteratisine	$C_{22}H_{33}NO_5$	391.24	7.29	0.02%
12	2,6-di-O-Galloyl-β-D-glucose	$C_{20}H_{20}O_{14}$	484.09	7.74	0.92%
13	Hetisine	$C_{20}H_{27}NO_3$	329.2	8.13	0.12%
14	3-O-Feruloylquinic acid	$C_{17}H_{20}O_9$	368.11	8.25	0.49%
15	Brevifolincarboxylic acid	$C_{13}H_8O_8$	292.02	8.68	0.86%
16	1,2,6-tri-O-Galloylglucose	$C_{27}H_{24}O_{18}$	636.1	9.43	0.58%
17	4-O-Feruloylquinic acid	$C_{17}H_{20}O_9$	368.11	9.45	0.16%
18	8-Oxohypecorinne	$C_{20}H_{15}NO_7$	381.08	9.68	0.75%
19*	Chebulanin	$C_{27}H_{24}O_{19}$	652.09	9.84	1.77%
20	3,5-di-O-Galloylshikimic acid	$C_{21}H_{18}O_{13}$	478.07	10.21	0.30%
21*	Corilagin	$C_{27}H_{22}O_{18}$	634.08	10.3	1.13%
22	Magnoflorine	$C_{20}H_{24}NO_4^+$	342.17	10.4	0.23%
23	6-Acetylheteratisine	$C_{24}H_{35}NO_6$	433.25	10.52	0.19%
24	Methyl gallate 3-O-β-D-(6'-O-Galloyl)-glucopyranoside	$C_{21}H_{22}O_{14}$	498.1	10.63	0.85%
25*	3,4,6-tri-O-Galloylglucose	$C_{27}H_{24}O_{18}$	636.1	10.78	1.58%
26	Leptopinine	$C_{20}H_{22}NO_6^+$	372.14	10.93	0.69%
27	Atisine	$C_{22}H_{33}NO_2$	343.25	11.05	0.24%
28*	1,3,6-tri-O-Galloylglucose	$C_{27}H_{24}O_{18}$	636.1	11.08	4.00%
29	5-O-Feruloylquinic acid	$C_{17}H_{20}O_9$	368.11	11.12	0.12%
30	Talatisamine	$C_{24}H_{39}NO_5$	421.28	11.14	0.39%
31	Neochebulinic acid or isomer	$C_{41}H_{34}O_{28}$	974.12	11.25	0.34%
32	1,3-di-O-Galloyl-2,4-chebuloylglucose	$C_{34}H_{28}O_{23}$	804.1	11.26	0.80%

(*Continued*)

https://doi.org/10.2147/DDDT.S505880

Table 2 (Continued).

Number	Name	Molecular Formula	Molecular Weight	Retention Time (min)	Comparative Content (%)
33	Methyl brevifolincarboxylate	$C_{14}H_{10}O_8$	306.04	11.79	0.21%
34	1,6-di-O-Galloyl-2,5-chebuloylglucose	$C_{34}H_{28}O_{23}$	804.1	12.3	0.32%
35*	Hypecorinine	$C_{20}H_{17}NO_6$	367.11	12.42	4.61%
36	Chasmanine	$C_{25}H_{41}NO_6$	451.29	12.47	0.06%
37	Neochebulinic acid or isomer	$C_{41}H_{34}O_{28}$	974.12	12.48	0.71%
38*	Chebulagic acid	$C_{41}H_{30}O_{27}$	954.1	12.67	2.20%
39	Quercetin 3-O-(2''-galloyl)-β-D-glucopyranoside	$C_{28}H_{24}O_{16}$	616.11	12.71	0.55%
40*	Leptopidine	$C_{20}H_{19}NO_6$	369.12	12.86	1.57%
41	Hypecocarpine	$C_{21}H_{23}NO_6$	385.15	12.9	0.51%
42*	Methyl neochebulinate or isomer	$C_{42}H_{36}O_{28}$	988.14	12.92	1.23%
43*	13-Oxocryptopine	$C_{21}H_{21}NO_6$	383.14	12.99	1.11%
44*	Ellagic acid	$C_{14}H_6O_8$	302.01	13.33	2.06%
45*	Hyperoside	$C_{21}H_{20}O_{12}$	464.1	13.56	2.90%
46	Quercetin 3-glucuronide	$C_{21}H_{18}O_{13}$	478.07	13.71	0.58%
47	14-O-Acetyltalatisamine	$C_{26}H_{41}NO_6$	463.29	13.73	0.63%
48*	Isoquercetin	$C_{21}H_{20}O_{12}$	464.1	13.82	1.50%
49*	Chebulinic acid	$C_{41}H_{32}O_{27}$	956.11	14.32	5.42%
50	Methyl neochebulinate or isomer	$C_{42}H_{36}O_{28}$	988.14	14.43	0.61%
51	Cryptopine	$C_{21}H_{23}NO_5$	369.16	14.47	0.43%
52*	Protopine	$C_{20}H_{19}NO_5$	353.13	14.68	3.01%
53	Kaempferol-3-O-rutinoside	$C_{27}H_{30}O_{15}$	594.16	14.74	0.47%
54*	Terchebin	$C_{41}H_{30}O_{27}$	954.1	15.02	2.52%
55*	Kaempferol 7-O-glucoside	$C_{21}H_{20}O_{11}$	448.1	15.23	1.12%
56	N-methylcanadine	$C_{21}H_{24}NO_4+$	354.17	15.42	0.19%
57*	Quercetin-7-O-β-D-glucoside	$C_{21}H_{20}O_{12}$	464.1	15.62	8.04%
58*	Astragalin	$C_{21}H_{20}O_{11}$	448.1	16.02	4.52%
59	N-methylstylopine	$C_{20}H_{20}NO_4+$	338.14	16.1	0.20%
60	4-O-(4''-O-Galloyl-α-L-rhamnopyranosyl ellagic acid	$C_{27}H_{20}O_{16}$	600.08	16.4	0.27%
61	Nantenine	$C_{20}H_{21}NO_4$	339.15	17.32	0.39%
62*	Quercetin 3-O-(6''-galloyl)-β-D-glucopyranoside	$C_{28}H_{24}O_{16}$	616.11	17.44	1.29%

(*Continued*)

Table 2 (Continued).

Number	Name	Molecular Formula	Molecular Weight	Retention Time (min)	Comparative Content (%)
63	Arjunoglucoside I	$C_{36}H_{58}O_{11}$	666.4	17.92	0.15%
64	Kaempferol 3-O-(6''-galloyl)-β-D-glucopyranoside	$C_{28}H_{24}O_{15}$	600.11	18.24	0.99%
65	Quercetin 3-O-(6''-O-p-coumaroyl)-glucoside	$C_{30}H_{26}O_{14}$	610.13	18.35	0.76%
66	Corydamine	$C_{20}H_{18}N_2O_4$	350.13	18.38	0.12%
67	Quercetin 3-O-(4''-O-p-coumaroyl)-glucoside	$C_{30}H_{26}O_{14}$	610.13	18.6	0.36%
68	Quercetin 3-O-(3''-O-p-coumaroyl)-glucoside	$C_{30}H_{26}O_{14}$	610.13	18.85	0.13%
69*	Quercetin	$C_{15}H_{10}O_7$	302.04	19.51	1.56%
70*	Tiliroside	$C_{30}H_{26}O_{13}$	594.14	19.9	1.39%
71	14-Benzoyltalatisamine	$C_{31}H_{43}NO_6$	525.31	20.16	0.11%
72	Kaempferol 3-O-(3''-O-p-coumaroyl)-glucoside	$C_{30}H_{26}O_{13}$	594.14	20.5	0.15%
73	Herpetrione	$C_{30}H_{32}O_{10}$	552.2	20.76	0.50%
74	Quercetin 3-O-(2''-O-p-coumaroyl)-glucoside	$C_{30}H_{26}O_{14}$	610.13	21.12	0.14%
75	$N^{1,N5,N10}$-tri-p-coumaroylspermidine	$C_{34}H_{37}N_3O_6$	583.27	21.72	0.83%
76	Hypecoumine	$C_{19}H_{11}NO_6$	349.06	22.03	0.02%
77	Kaempferol	$C_{15}H_{10}O_6$	286.05	22.48	0.54%
78	Indaconitine	$C_{34}H_{47}NO_{10}$	629.32	22.74	0.36%
79	Yunnaconitine	$C_{35}H_{49}NO_{11}$	659.33	22.96	0.31%
80	Herpetetrone	$C_{40}H_{42}O_{13}$	730.26	23.15	0.12%
81	Trihydroxyoctadecenoic acid	$C_{18}H_{34}O_5$	330.24	23.54	0.96%
82	Sericic acid	$C_{30}H_{48}O_6$	504.35	24.1	0.36%
83*	Arjungenin	$C_{30}H_{48}O_6$	504.35	24.23	2.48%
84	Terminolic acid	$C_{30}H_{48}O_6$	504.35	25.32	0.57%
85	Dihydroxyoctadecadienoic acid or isomer	$C_{18}H_{32}O_4$	312.23	25.67	0.41%
86	Dihydroxyoctadecadienoic acid or isomer	$C_{18}H_{32}O_4$	312.23	25.78	0.69%
87	Isosakuranetin	$C_{16}H_{14}O_5$	286.08	26.22	0.60%
88	Herpetolide B	$C_{16}H_{12}O_6$	300.06	26.31	0.43%
89*	9-Hydroperoxy-10E,12,15Z-octad ecatrienoic acid	$C_{18}H_{30}O_4$	310.21	26.68	1.31%
90	Arjunolic acid	$C_{30}H_{48}O_5$	488.35	26.86	0.13%

(*Continued*)

https://doi.org/10.2147/DDDT.S505880

Table 2 (Continued).

Number	Name	Molecular Formula	Molecular Weight	Retention Time (min)	Comparative Content (%)
91	Arjunic acid	$C_{30}H_{48}O_5$	488.35	27.74	0.27%
92	Corchorifatty acid D	$C_{18}H_{28}O_4$	308.2	28.26	0.47%
93*	Hydroxylinoleic acid	$C_{18}H_{32}O_3$	296.24	30.74	1.67%
94	Maslinic acid	$C_{30}H_{48}O_4$	472.36	31.38	0.14%

Note: "*"Relative content greater than 1%.

SYW Reduces LPS-Induced Inflammation

LPS is an activator of innate immune response that can trigger inflammation in zebrafish. In Figures 2C and F, the fluorescent cell counts in the LPS-treated zebrafish were greatly increased in comparison to that in the control group ($P < 0.01$). Compared with that in the model group, the IOD in the SYW treatment group (25, 50, and 100 μg/mL) was lower ($P < 0.01$), suggesting that SYW exhibited anti-inflammatory activity.

Anti-Inflammatory Activity of SYW in vitro

To investigate the cytotoxic effects of SYW on RAW264.7 cells, a CCK8 assay was utilized. Our results showed that SYW promoted cell proliferation at a concentration of 1.25, 2.5, and 5 μg/mL, whereas significant cytotoxicity was observed at 25 and 50 μg/mL (Figure 3A). Hence the concentrations of SYW at 1.25, 2.5, 5, and 10 μg/mL were used to detect anti-inflammatory activity. No, TNF-α, IL-6, and IL-1β are classical inflammatory markers, we measured their content. LPS led to a significant rise in nitrite concentration, which was dose-dependently reversed by SYW (Figure 3B).

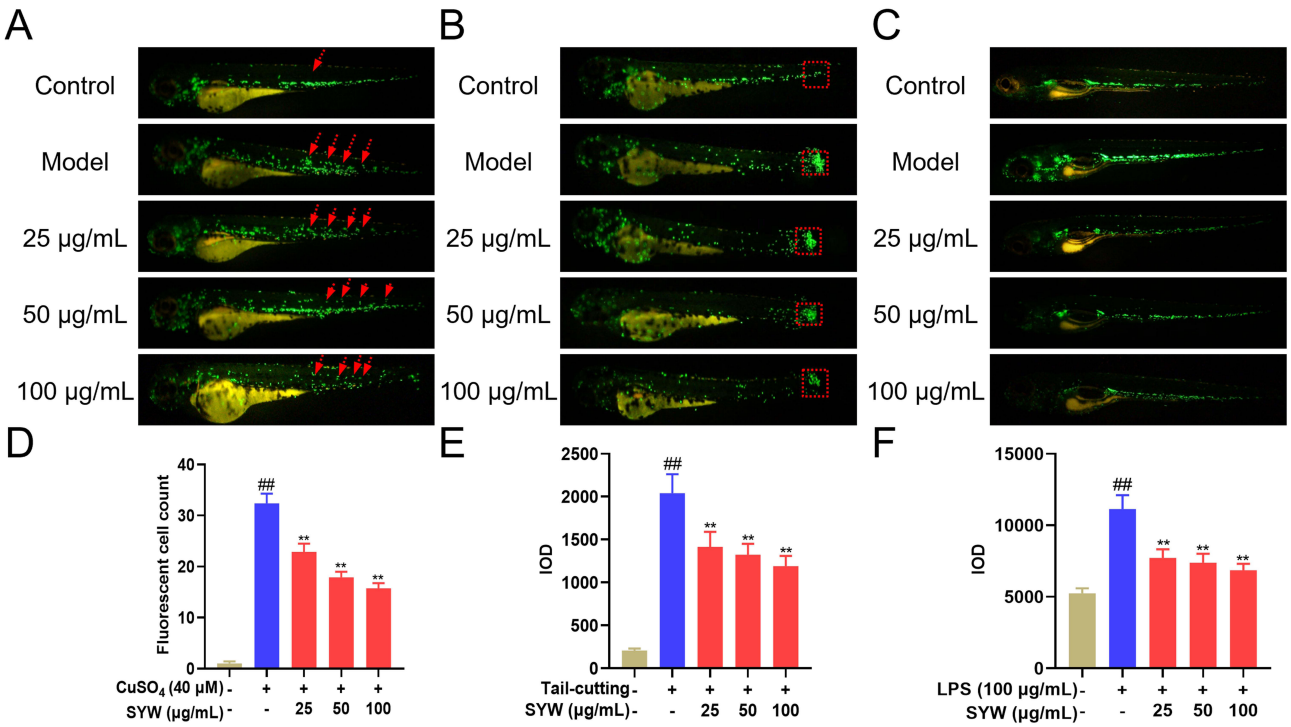

Figure 2 (**A**) SYW restrained $CuSO_4$-induced inflammatory cell migration in zebrafish. The red arrow indicates the inflammatory cells at the lateral line. n = 8. (**B**) SYW inhibited tail-cutting-induced inflammatory cell aggregation. The red box area indicates the inflammatory cells that accumulated at the wound. n = 6. (**C**) SYW treatment ameliorated LPS-induced inflammation. n = 10. (**D–F**) show the statistical analysis of (**A–C**). All experiences were performed at least 3 times and data were expressed as mean ± SEM. $^{\#\#}P < 0.01$ in contrast to the control group; $^{**}P < 0.01$ in contrast to the model group.

 https://doi.org/10.2147/DDDT.S505880

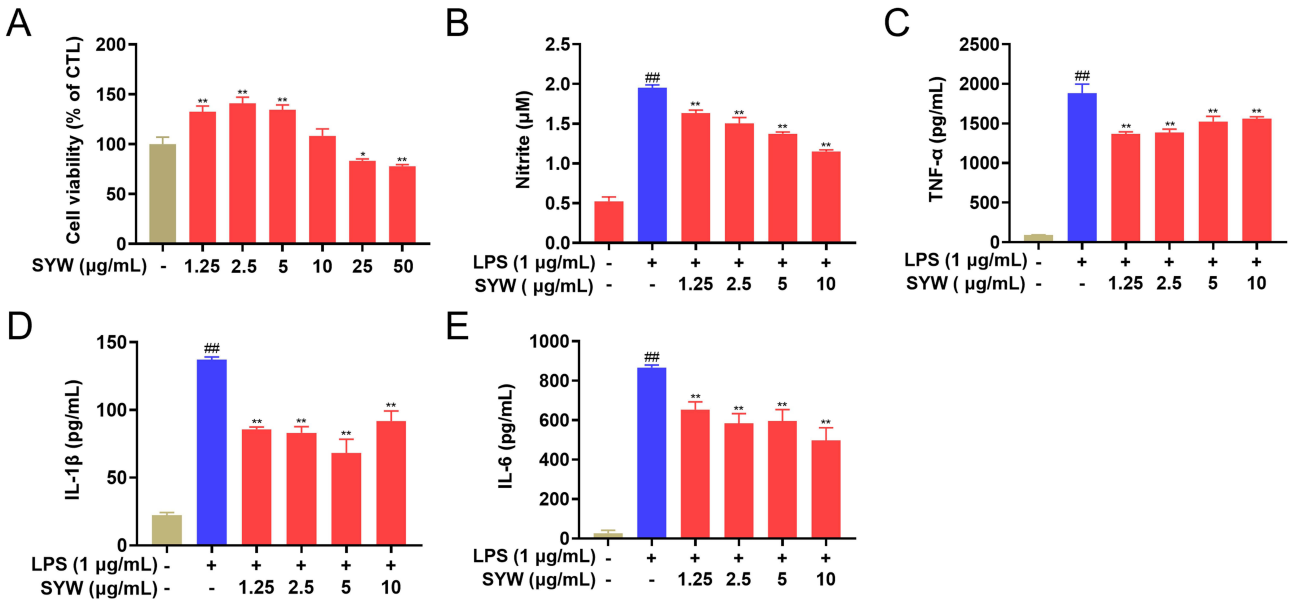

Figure 3 (**A**) Cell viability in the different SYW concentration groups. n = 6. *P < 0.05, **P < 0.01 in contrast to the control group. (**B**) Effect of SYW on the nitrite density. (**C**) The concentration of TNF-α. (**D**) The concentration of IL-1β. (**E**) The concentration of IL-6. n = 5. All experiences were performed at least 3 times and data were expressed as mean ± SEM. ##P < 0.01 in contrast to the control group; **P < 0.01 in contrast to the LPS group.

Additionally, ELISA analysis indicated that LPS stimulated the release of TNF-α, IL-1β, and IL-6. However, treatment with SYW reduced the concentration of TNF-α, IL-1β, and IL-6 (P < 0.01) (Figure 3C–E).

Results of Network Pharmacology

SYW-Targets-Cholecystitis Network Construction

To clarify determine the anti-cholecystitis mechanism of SYW, we constructed a network depicting SYW-Targets-Cholecystitis. Initially, 712 potential targets of SYW were identified. With the keyword cholecystitis, we obtained 798 disease targets. Afterward, through Venn analysis, a total of 106 potential SYW targets for cholecystitis were screened (Figure 4A). Figure 4B shows that a visual network diagram of SYW-Targets-Cholecystitis was constructed by Cytoscape. It contained 133 nodes and 1517 edges. The middle green triangle represents diseases. The triangle, red

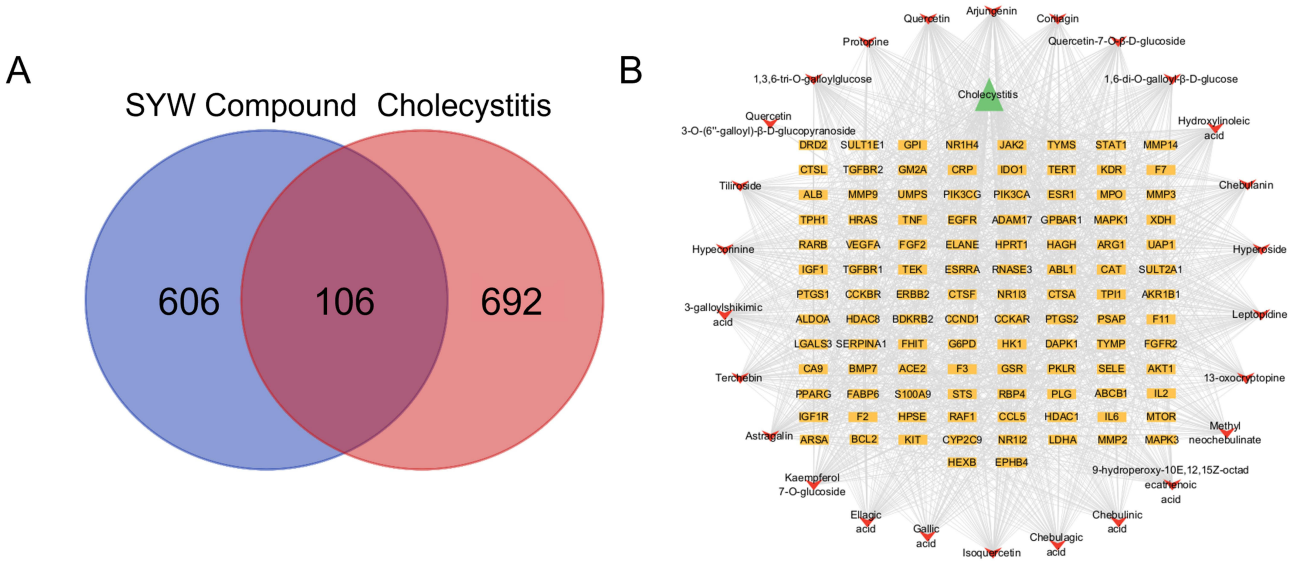

Figure 4 (**A**) Venn graph of the interaction between SYW and cholecystitis. (**B**) SYW-Targets-Cholecystitis visual network diagram.

https://doi.org/10.2147/DDDT.S505880

nodes represent 26 chemical components. And rectangle, yellow nodes represent the targets associated with the anti-cholecystitis effects of SYW, such as IL6, TNF, and AKT1.

Construction of the PPI Network

We further drew the PPI network to investigate the interaction landscape. Figure 5A shows that the PPI network had 106 nodes and 1163 edges. The PPI network analysis revealed a total of 106 genes. The degree value is represented by the node's size. The subnetworks were extracted by taking the median value of DC, BC, and CC as thresholds, and resulting in a PPI network with 16 nodes and 112 edges (Figure 5B). The targets in subnetworks were identified as the hub genes, and the relationship between SYW components and these genes was explored (Supplementary Data 1). The key genes (degree ≥ 50) included ALB, IL6, TNF, AKT1, EGFR, MMP9, BCL2, ESR1, PPARG, and MAPK3. These targets might strongly correlate with cholecystitis.

GO and KEGG Enrichment Analysis

For GO enrichment, 125 terms were screened (p value ≤ 0.01 and FDR ≤ 0.05). Among the 125 terms, 79 were related to biological process (BP), 20 were related to cellular component (CC), and the remaining 26 were related to molecular function (MF). BP entries are mainly associated with the positive regulation of protein kinase B signaling, positive regulation of PI3K signaling, positive regulation of the MAPK cascade, protein autophosphorylation, and the insulin-like growth factor receptor signaling pathway. In CC entries, SYW mainly regulated extracellular space and receptor complexes. In MF entries, the effect of SYW was associated with the regulation of protein serine/threonine/tyrosine kinase activity, transmembrane receptor protein tyrosine kinase activity, protein kinase activity, etc (Figure 6A).

A total of 103 signaling pathways were subjected to KEGG enrichment analysis (p value ≤ 0.01 and FDR ≤ 0.05). Figure 6B shows that these pathways are more associated with inflammation and immunity, including PI3K-Akt, FoxO, AGE-RAGE, and HIF-1 signaling pathways, as well as EGFR tyrosine kinase inhibitor resistance. Among the hub genes, the PI3K-AKT and FoxO signaling pathways enriched the largest number of genes. Therefore, the PI3K/AKT/FoxO signaling pathway is noted as the crucial pathway of SYW for cholecystitis treatment. The targets enriched in PI3K-Akt and FoxO signaling pathways are shown in Figures 6C and D.

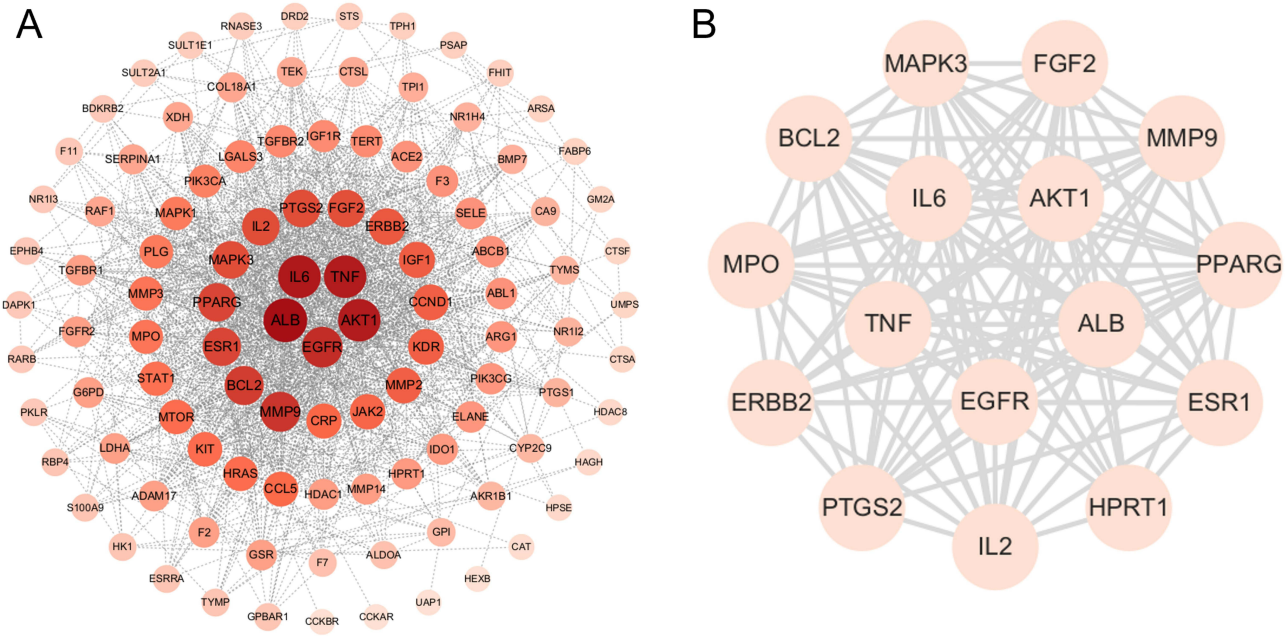

Figure 5 (**A**) The protein-protein interaction (PPI) network. (**B**) The 16 hub genes of SYW against cholecystitis.

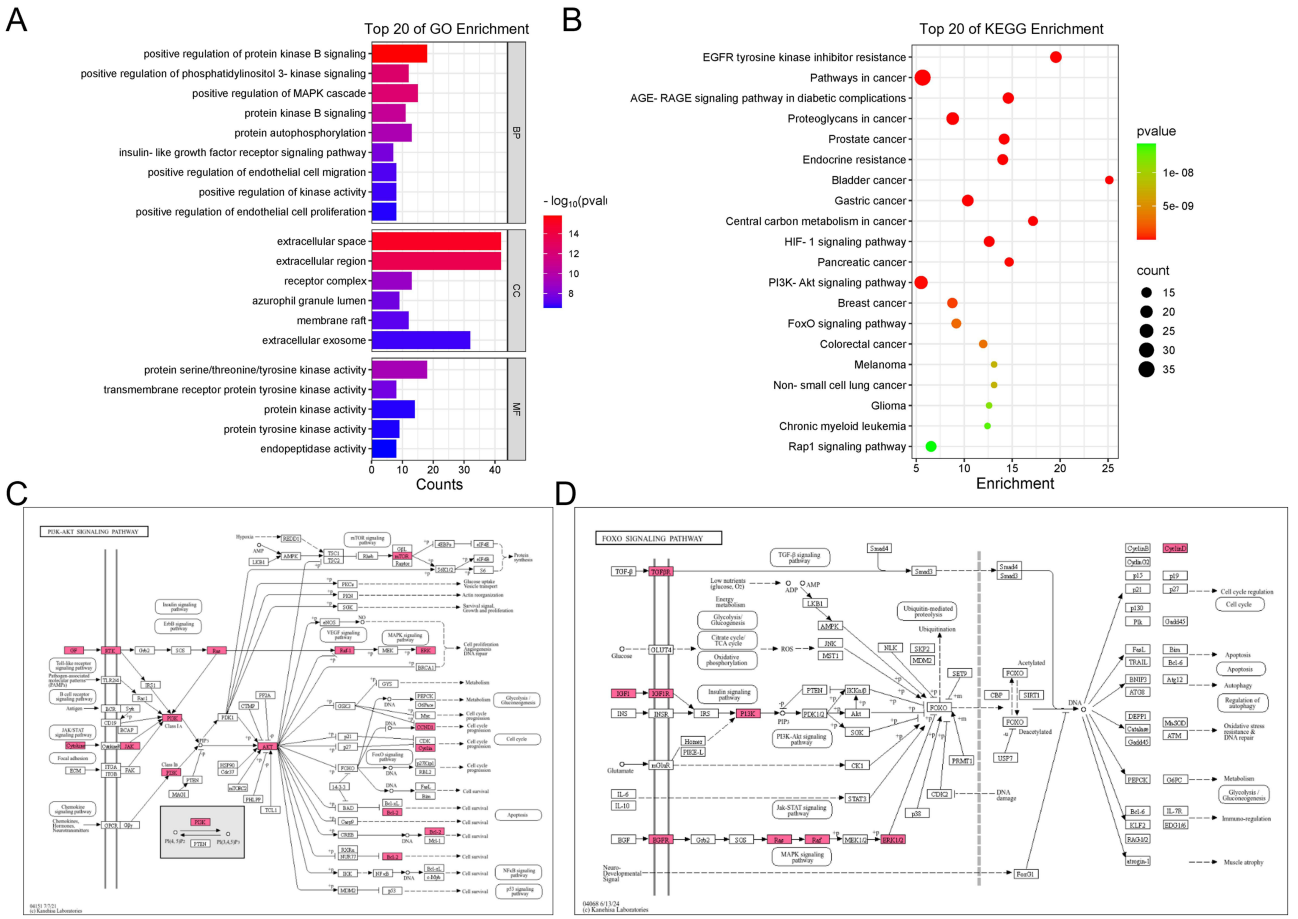

Figure 6 (**A**) The results of GO enrichment analysis. (**B**) The results of KEGG pathway enrichment analysis. (**C**) The PI3K-AKT signaling pathway map, red nodes represent relevant genes participating in regulation. (**D**) The FoxO signaling pathway map, red nodes represent relevant genes participating in regulation.

Expression Level of Genes

As described above, the PI3K/Akt/FoxO signaling pathways and the anti-inflammation targets, such as IL6, TNF, AKT1, and EGFR, may involved in the anti-cholecystitis mechanism of SYW. In this part, the relevant gene expression levels were detected to verify the network pharmacology results. First, eleven genes that enriched in PI3K/Akt/FoxO signaling pathways were tested. As shown in Figure 7A–K, *vegf, irs1, il7ra, il6, mapk3, pik3ca, akt1, foxo1*, and *bcl6* were upregulated, and *hras* was downregulated in zebrafish with inflammation, whereas SYW treatment rescued the expression. Furthermore, mRNA levels of genes with high-degree values in the PPI network, including *egfr1, mmp9, esr1, ptgs2*, and *il1β* were also detected. As shown in Figure 7L–P, compared to the control group, the genes were upregulated in zebrafish with inflammation. Compared to the model group, SYW treatment downregulated the expression of these genes. Detail results can be found in Supplementary Data 2.

Discussion

SYW, a traditional TTM formula, has been widely used to treat cholecystitis and hepatitis with a definite curative effect. However, its chemical composition, modern pharmacological effects, and potential mechanisms remain unknown. In this research, we conducted an analysis of the chemical composition of SYW using UPLC-Q-TOF/MS, and assessed its anti-inflammatory effects in zebrafish and cells. Furthermore, network pharmacological analysis and qRT–PCR were performed to investigate the underlying mechanisms.

SYW is composed of 11 traditional Tibetan medicinal materials, including mainly herbal materials, animal-based and mineral-based medicines. The animal source medicine is Moschus and Heibingpian in this formula. Moschus has a medicinal history of more than 2000 years. In order to strengthen the protection of endangered animals, artificial

https://doi.org/10.2147/DDDT.S505880

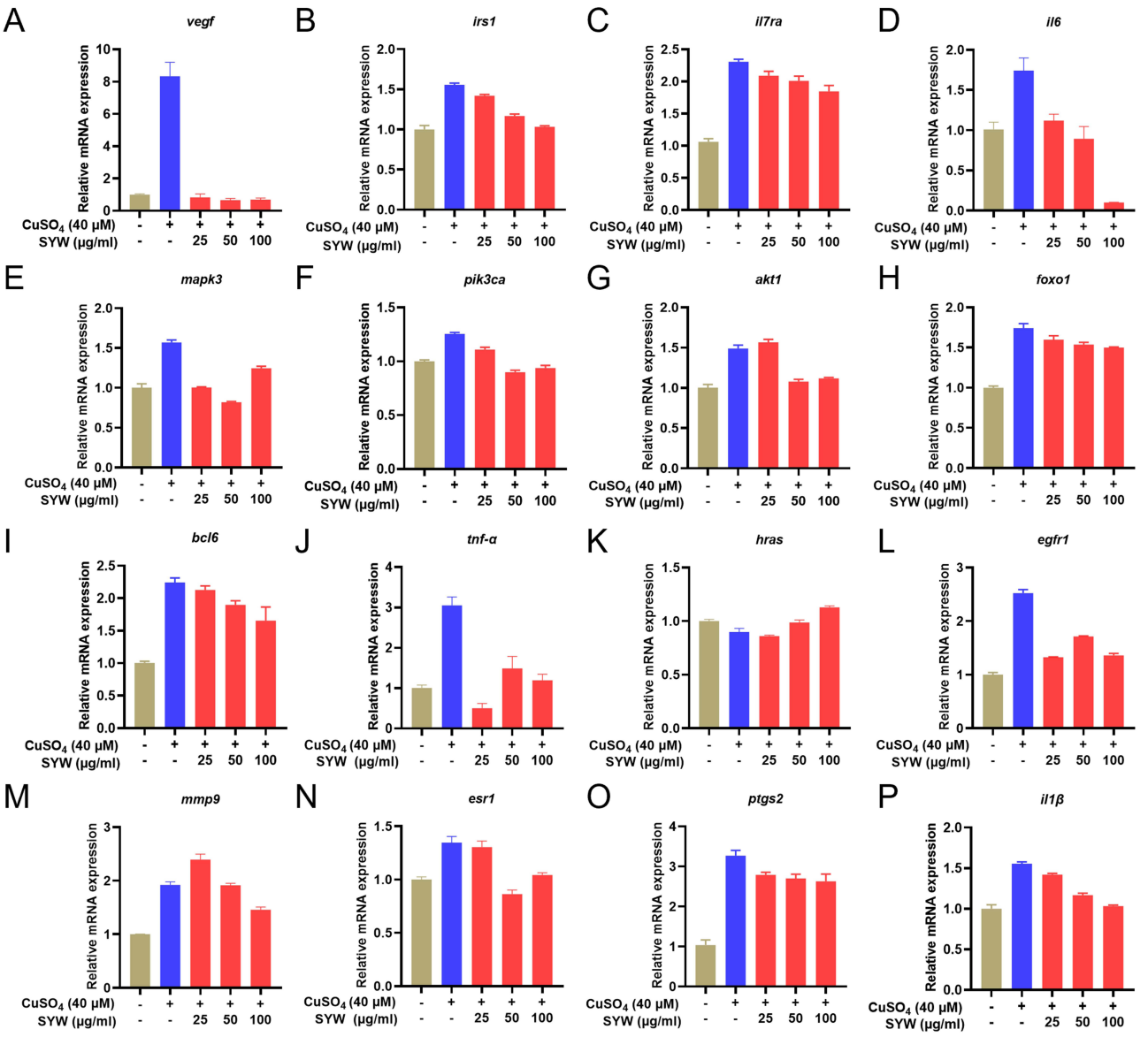

Figure 7 Effect of SYW on the expression levels of inflammation-related genes in zebrafish. (**A**) *vegf*. (**B**) *irs1*. (**C**) *il7ra*. (**D**) *il6*. (**E**) *mapk3*. (**F**) *pik3ca*. (**G**) *akt1*. (**H**) *foxo1*. (**I**) *bcl6*. (**J**) *tnf-α*. (**K**) *hras*. (**L**) *egfr1*. (**M**) *mmp9*. (**N**) *esr1*. (**O**) *ptgs2*. (**P**) *il1β*. n = 3. All experiences were performed at least 3 times and data were expressed as mean ± SEM.

musk with similar pharmacological effects and physical properties to moschus, has been used to replace moschus in SYW. In addition, Heibingpian belongs to animal fecal medicines. Fecal medicines play an important position in traditional Tibetan medical systems. Heibingpian is used to treat dyspepsia and gastric ulcers in the nineteenth century, demonstrating efficacy in strengthening the stomach and gallbladder. The medicinal components of SYW have been clearly defined, but the chemical composition of SYW and the 11 Tibetan medicines in the SYW formula, are rarely reported. Here, by UPLC-Q-TOF/MS analysis, 94 compounds were recognized from SYW. The major types of compounds included alkaloids, phenols, phenolic acids, flavonoids, and terpenoids. Screening of potential pharmacodynamic substances plays a crucial role in the development of drugs. In general, compounds with higher relative content can be identified more accurately and with some reproducibility, and are more likely to be the main pharmacoactive substance. Previous studies have shown that a relative content threshold greater than 1% is an appropriate screening criterion.[22] In our study, 28 compounds had a relative content of more than 1%, which might be the main potential pharmacodynamic substances of SYW, such as gallic acid, chebulinic acid, quercetin-7-O-β-D-glucoside, and hypecorinine. However, the composition of Tibetan medicine is extremely complex, potentially containing compounds with

a relative content of less than 1% that exhibit significant medicinal effects. Therefore, the exact pharmacodynamic substance of SYW needs to be further isolated and verified.

Relieving gallbladder inflammation is the basic treatment for cholecystitis. Whether SYW works to treat cholecystitis by relieving inflammation remains unclear. In our study, we used three zebrafish inflammation models and a cell model to evaluate the anti-inflammatory effect of SYW. $CuSO_4$ expression can selectively damage the sensory hair cell population at lateral line neuromast cells, inducing an acute inflammatory response.[23] In this model, when inflammation occurs, the migration of immune cells to the lateral line can be visually observed and quantified. Our results showed that the number of immune cells close to the lateral line was significantly decreased in the SYW treatment groups. Tail-cutting can induce acute inflammation with an accumulation of immune cells near the cutting area.[24] Our study showed that SYW treatment alleviated the accumulation of immune cells. Infectious inflammation in zebrafish is usually established by LPS culture water exposure or injection.[25] As shown in Figure 2C, the immune cells in SYW-treated zebrafish became sparse. In the cell model, SYW reduced the LPS-induced NO production and decreased the concentrations of IL-1β, IL-6, and TNF-α. Overall, these results demonstrated that SYW inhibited inflammatory responses in zebrafish and in vitro.

The combination of network pharmacology and qRT–PCR technology provides an effective means for rapidly elucidating the mechanism of traditional medicinal action. In this study, we focused on the main compounds with a relative content greater than 1% to predict the targets of SYW, except for two compounds (3-di-O-galloyl-β-D-glucose and 3,4,6-tri-O-galloylglucose), for which no target information could be found. It has been revealed that some of the 26 compounds have definite anti-inflammatory properties. For example, gallic acid suppressed the expression of inflammatory factors and blocked the NF-κB pathway, thereby playing its anti-inflammatory effects.[26] Choleric acid demonstrated anti-inflammatory properties by suppressing the production of NO and PGE2 and downregulating iNOS, COX-2, 5-LOX, TNF-α, and IL-6.[27] Ultimately, 106 possible targets for SYW in cholecystitis treatment were collected. The PPI network indicated that ALB, IL-6, AKT1, TNF, EGFR, MMP9, BCL-2, PPARG, and ESR1 were important targets of SYW. ALB has antioxidative, anti-inflammatory, and antiapoptotic effects. Moreover, it can reduce enteritis by inhibiting the NF-κB/NLRP3 signaling pathway.[28] IL6 is involved in inflammation and exerts regulatory effects through the NF-κB and PI3K pathways.[29] AKT1 is essential in the PI3K/AKT pathway and serves as an essential upstream regulator of the NLRP3 inflammasome.[30] Decreasing TNF-α can effectively inhibit NF-κB activation and macrophage-mediated inflammation.[31] The EGFR signaling pathway is associated with the regulation of inflammation, in which EGFR plays a key role.[32] MMP9 was reported to regulate inflammation through the PI3K/Akt and MAPK/ERK signaling pathways.[33] BCL2 is a highly regulated target gene of NF-κB that can promote the survival and inflammation of selected leukocyte subsets.[34] PPARg, a master regulator of adipogenesis, modulates macrophage differentiation and polarization.[35] In addition, variants in the ESR1 gene have been associated with inflammation.[36] In summary, SYW is likely to ameliorate inflammation via multiple targets.

The results of GO enrichment demonstrated that the majority of the entries are linked to the regulation of metabolic processes, signal transduction, and cell migration and proliferation responses. According to the KEGG pathway analysis, the anti-inflammatory effect of SYW has strong associations with the PI3K-Akt, FoxO, HIF-1 pathways, and EGFR tyrosine kinase inhibitor resistance. Among the hub genes, the PI3K-AKT and FoxO signaling pathways enriched the largest number of genes. Clinical studies have shown that 8.6% of patients with chronic cholecystitis have positive staining for PI3K.[37] PI3K activation enhances TNF-α and IL-6 synthesis, which further drives the inflammatory response.[38] AKT, as a downstream signaling molecule, is activated by PI3K to regulate cell function. AKT activation can phosphorylate and inactivate transcription factors such as NF-κB. By inhibiting NF-κB activation, AKT reduces the production of pro-inflammatory cytokines, thereby dampening the inflammatory response. FoxO activity is affected by the upstream signal pathway PI3K/AKT, and regulates the expression of inflammation-related genes, such as IL-1β and TLR4 in macrophages, affecting the inflammatory response.[39,40] Therefore, the PI3K/AKT/FoxO signaling pathway has a significant impact on inflammation. And inhibition of PI3K activity can effectively reduce inflammatory response and ameliorate disease symptoms.[41]

Network pharmacology intuitively reveals the relationship between the components, targets of SYW and cholecystitis, and fully demonstrates the characteristics of multi-components, multi-targets, and multi-pathways of TTM to play a therapeutic role. However, the current study also exposed some limitations of the network pharmacology. For example, the database of obtaining targets is not perfect, and the reliability of the data and analysis results need to be further verified. And the screening

criteria for active substances need to be optimized. To solve this drawback, we can combine serum pharmacochemistry, network pharmacology, and experimental verification, so as to improve the accuracy of the results.

In zebrafish, $CuSO_4$ treatment significantly increased the expression levels of *vegf*. SYW can efficiently inhibit the expression of this gene. VEGF can promote the aggregation of inflammatory cells, and inhibition of VEGF can effectively inhibit inflammatory response.[42] In addition, VEGF can activate phosphoinositide 3-kinase (PI3K).[43] PI3K can promote PIP3 translate into PIP2, so then block downstream target Akt.[44] In this study, SYW restored the expression level of *irs1, il6, mapk3, pik3ca, akt1*, and *hras* induced by $CuSO_4$. These findings suggested that SYW could down-regulate the expression of these genes to control the PI3K-Akt pathway. In addition, research has indicated that FoxO transcription factor family is pivotal in a pathway downstream of PI3K-AKT.[45] According to the present study, $CuSO_4$ can successfully suppress the expression of important FoxO pathway genes, including *foxo1, bcl6, il7ra*, and *tnf-α*. Similarly, SYW can effectively downregulate the expression of these genes. The FoxO pathway ultimately affects apoptosis, autophagy, and the cell cycle. Therefore, by controlling the FoxO pathway, SYW may have an impact on the death and growth of inflammatory cells. FoxO is a transcription factor that regulates adipose inflammation in mammals. It can promote the inflammatory cascade in adipose tissue and affect immune system homeostasis.[46] Furthermore, as the downstream gene target of FoxO1, il1β was significantly influenced by it.[47] The qRT–PCR results demonstrated that SYW can dose-dependently reduce the expression level of *il1β* in zebrafish, thereby mitigating inflammation. Moreover, we detected the mRNA levels of several inflammatory genes (*egfr1, esr1, mmp9*, and *ptgs2*) as well. The results demonstrated that SYW significantly lowered the expression levels of *egfr1, esr1, mmp9*, and *ptgs2*. Studies have shown that blocking EGFR signaling can effectively reduce the release of proinflammatory cytokines.[48] EGFR can reduce the inflammatory response and apoptosis of H9c2 cells.[49] And many inflammatory illnesses have been due to variants in the ESR1 gene.[36] MMP9 ameliorates periosteal cell differentiation by mediating the inflammatory response and the distribution of inflammatory cells.[50] Another study demonstrated that downregulation of PTGS2 can reduce joint swelling and the arthritis index in rats.[11] These findings align with the results observed in the present study. Hence, our results may imply that SYW showed anti-cholecystitis effects by PI3K/AKT/FoxO signaling pathways. A concrete visualization mechanism diagram of SYW intervention in cholecystitis is shown in Figure 8.

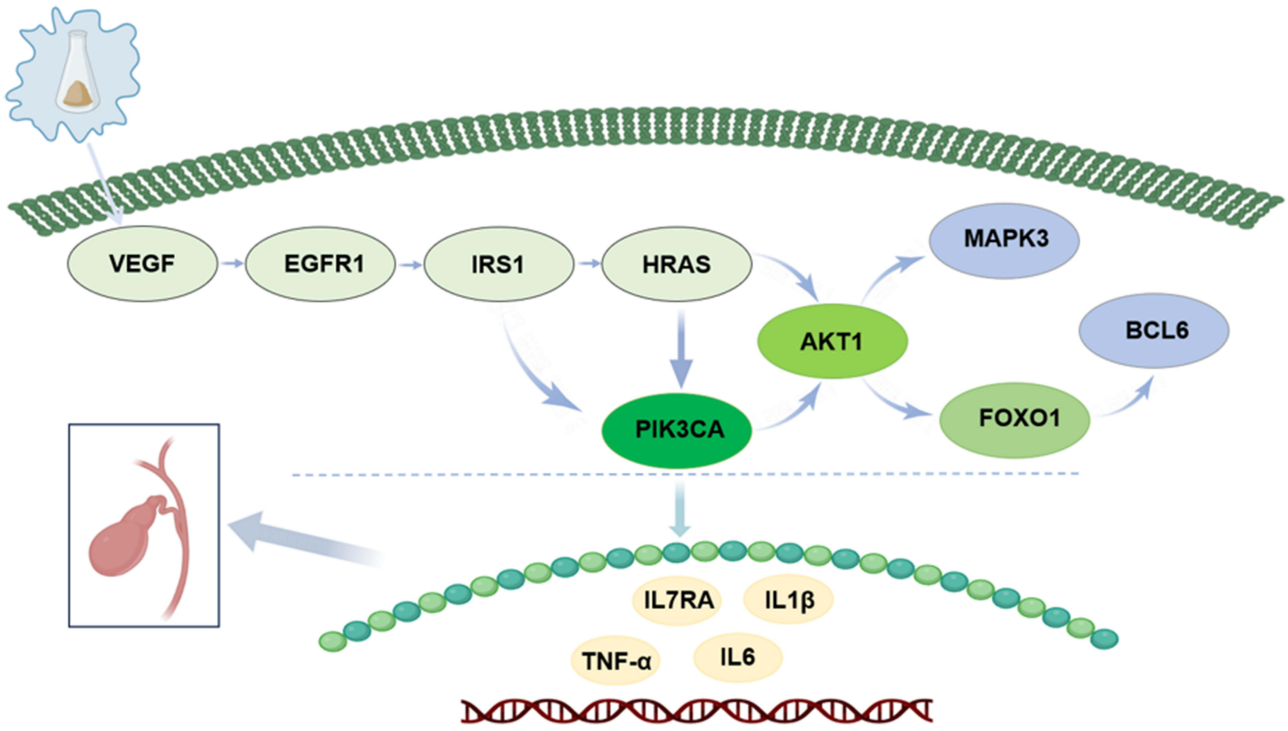

Figure 8 A conceptual framework describing the potential mechanism by which SYW in the treatment of cholecystitis.

Zebrafish and cell models are mainly used for this research. Recently, the zebrafish model has been recognized as an optimal model for drug evaluation with biological complexity, cycle shortly, and high-throughput characteristics.[51] However, the PI3K/Akt/FoxO signaling pathway is more dependent on its phosphorylation, and the lack of related antibodies against zebrafish PI3K/Akt/FoxO signaling pathway imposes an obstacle to support our conclusion. In the future, further validation using cell and rat models is necessary to substantiate this conclusion.

Conclusion

Our study first identified 94 components of SYW by UPLC-Q-TOF/MS. The results of three zebrafish inflammation models showed that SYW could effectually suppress the migration and growth of inflammatory cells. SYW was also found to inhibit the release of inflammatory factors in the RAW264.7 cell model. Furthermore, network pharmacology analysis identified ALB, IL6, TNF, AKT1, and EGFR as potential key targets of SYW. KEGG enrichment and qRT–PCR analysis showed that the PI3K/Akt/FoxO signaling pathway played a role in the anti-inflammatory effects of SYW. This research offers a theoretical basis and reference for the further development and utilization of SYW.

Abbreviations

TTM, traditional Tibetan medicine; SYW, Shiyiwei golden Pill; UPLC-Q-TOF/MS, ultrahigh-performance liquid chromatography with quadrupole time-of-flight mass spectrometry; LPS, lipopolysaccharide; CCK-8, Cell counting kit-8; dpf, days post fertilization; GO, Gene ontology; KEGG, Kyoto encyclopedia of genes and genomes; qRT–PCR, quantitative real-time polymerase chain reaction.

Data Sharing Statement

Data used to support the findings of this study are available from the corresponding author upon request.

Ethical Approval

The study protocol was approved by the Ethics Committee of Shandong Academy of Sciences (SWS20230427).

Acknowledgments

We would like to thank all the participants involved in this research for their time and contributions.

Author Contributions

All authors made a significant contribution to the work reported, whether that is in the conception, study design, execution, acquisition of data, analysis and interpretation, or in all these areas; took part in drafting, revising or critically reviewing the article; gave final approval of the version to be published; have agreed on the journal to which the article has been submitted; and agree to be accountable for all aspects of the work.

Funding

This work was supported by the National Key R&D Program of China (2022YFC2804600), the Basic and Talent Research Project of the Pilot Project for the Integration of Science, Education and Industry, Qilu University of Technology, Shandong Academy of Sciences (2023RCKY229), the 2021 Doctoral Program Construction Project of Traditional Chinese Medicine (Tibetan Medicine) of Tibetan traditional medicine college (BSDPY-21-13), Shandong Provincial Central Guidance Local Science and Technology Development Fund Project (YDZX2022164), Innovation Ability Improvement Project of Science and Technology of Small and Medium-size Enterprise in Shandong Province (2022TSGC2003).

Disclosure

The authors declare no competing interests in this work.

References

1. Zhu Z, Li F, Hu K, et al. An epidemiological survey of gallbladder diseases in Zhenhai District, Ningbo. *Mod Pract Med*. 2012;2012(11):47–48. doi:10.3969/j.issn.1671-0800.2012.11.021
2. Lyv F, Ding D, Liu J, et al. An epidemiological investigation of cholecystitis for the nationality of Uygur, Han, and Kazak in Xinjiang. *Lab Med Clin*. 2019;16(09):1191–1195. doi:10.3969/j.issn.1672-9455.2019.09.011
3. Zheng Z, Xiong H, Zhao Z, et al. Tibetan medicine Si-Wei-Qiang-Wei Powder ameliorates cholecystitis via inhibiting the production of pro-inflammatory cytokines and regulating the MAPK signaling pathway. *J Ethnopharmacol*. 2023;303:116026. doi:10.1016/j.jep.2022.116026
4. Pan L, Gao J, Han Y, et al. The treatment of cholecystitis and cholelithiasis by Tibetan Medicine. *Evid Based Complement Alternat Med*. 2021;2021:1–21. doi:10.1155/2021/9502609
5. Dhondup L, Husted C. Tibetan medicine and regeneration. *Ann NY Acad Sci*. 2009;1172(1):115–122. doi:10.1111/j.1749-6632.2009.04500.x
6. Geng Z, Ao J. Clinical observation of zang medicine treatment of chronic cholecystitis. *E JClin Med Literature*. 2018;5(87):157–158. doi:10.16281/j.cnki.jocml.2018.87.138
7. Li J. Clinical observation on 54 cases of chronic cholecystitis treated by combining Tibetan and western medicine. *Chin J Ethnomedicine Ethnopharm*. 2016;25(10):1,7.
8. Ou L, Liu HR, Shi XY, et al. Terminalia chebula Retz. aqueous extract inhibits the Helicobacter pylori-induced inflammatory response by regulating the inflammasome signaling and ER-stress pathway. *J Ethnopharmacol*. 2024;320:117428. doi:10.1016/j.jep.2023.117428
9. Kim HJ, Song HK, Park SH, et al. *Terminalia chebula Retz*. extract ameliorates the symptoms of atopic dermatitis by regulating anti-inflammatory factors in vivo and suppressing STAT1/3 and NF-κB signaling in vitro. *Phytomedicine*. 2022;104:154318. doi:10.1016/j.phymed.2022.154318
10. Koyuncu AG, Cumbul A, Noval MKA, et al. Pomegranate seed oil alleviates colitis: therapeutic effects achieved by modulation of oxidative stress and inflammation in a rat model. *Prostaglandins Other Lipid Mediat*. 2024;173:106837. doi:10.1016/j.prostaglandins.2024.106837
11. Wei X, Fan X, Feng Z, et al. Ethyl acetate extract of herpetospermum pedunculosum alleviates α-naphthylisothiocyanate-induced cholestasis by activating the farnesoid x receptor and suppressing oxidative stress and inflammation in rats. *Phytomedicine*. 2020;76:153257. doi:10.1016/j.phymed.2020.153257
12. Zhang GQ, Huang XD, Wang H, et al. Anti-inflammatory and analgesic effects of the ethanol extract of Rosa multiflora Thunb. hips. *J Ethnopharmacol*. 2008;118(2):290–294. doi:10.1016/j.jep.2008.04.014
13. Guo D, Xu L, Cao X, et al. Anti-inflammatory activities and mechanisms of action of the petroleum ether fraction of Rosa multiflora Thunb. hips. *J Ethnopharmacol*. 2011;138(3):717–722. doi:10.1016/j.jep.2011.10.010
14. Chen T, Wang X, Chen P, et al. Chemical components analysis and in vivo metabolite profiling of Jian'er Xiaoshi oral liquid by UHPLC-Q-TOF-MS/MS. *J Pharm Biomed Anal*. 2022;211:114629. doi:10.1016/j.jpba.2022.114629
15. Tai J, Ye C, Cao X, et al. Study on the anti-gout activity of the lotus seed pod by UPLC-QTOF-MS and virtual molecular docking. *Fitoterapia*. 2023;167:105500. doi:10.1016/j.fitote.2023.105500
16. Zhang Y, Xia Q, Wang J, et al. Progress in using zebrafish as a toxicological model for traditional Chinese medicine. *J Ethnopharmacol*. 2022;282:114638. doi:10.1016/j.jep.2021.114638
17. Liu C, Fan FF, Li XH, et al. Elucidation of the mechanism of action of the anticholecystitis effect of the Tibetan medicine "Dida" using network pharmacology. *Trop J Pharm Res*. 2020;19(7):1449–1457. doi:10.4314/tjpr.v19i7.17
18. Fleige S, Pfaffl MW. RNA integrity and the effect on the real-time qRT-PCR performance. *mol Aspect Med*. 2006;27(2–3):126–139. doi:10.1016/j.mam.2005.12.003
19. Wu J, Zhang F, Ruan H, et al. Integrating network pharmacology and RT-qPCR analysis to investigate the mechanisms underlying zexie decoction-mediated treatment of non-alcoholic fatty liver disease. *Front Pharmacol*. 2021;12:722016. doi:10.3389/fphar.2021.722016
20. Hamieau M, Loulergue P, Szydłowska-Czerniak A. Green solvent extraction of antioxidants from herbs and agro-food wastes: optimization and capacity determination. *Appl Sci*. 2024;14(7):2936. doi:10.3390/app14072936
21. Livak KJ, Schmittgen TD. Analysis of relative gene expression data using real-time quantitative PCR and the $2^{-\Delta\Delta CT}$ method. *Methods*. 2001;25(4):402–408. doi:10.1006/meth.2001.1262
22. Zhou C, Chen J, Zhang H, et al. Investigation of the chemical profile and anti-inflammatory mechanisms of flavonoids from Artemisia vestita wall. ex besser via targeted metabolomics, zebrafish model, and network pharmacology. *J Ethnopharmacol*. 2023;302:115932. doi:10.1016/j.jep.2022.115932
23. d'Alençon CA, Peña OA, Wittmann C, et al. A high-throughput chemically induced inflammation assay in zebrafish. *BMC Biol*. 2010;8(1):151. doi:10.1186/1741-7007-8-151
24. Xie Y, Meijer AH, Schaaf MJM. Modeling Inflammation in zebrafish for the development of anti-inflammatory drugs. *Front Cell Dev Biol*. 2021;8:620984. doi:10.3389/fcell.2020.620984
25. Watzke J, Schirmer K, Scholz S. Bacterial lipopolysaccharides induce genes involved in the innate immune response in embryos of the zebrafish (Danio rerio). *Fish Shellfish Immunol*. 2007;23(4):901–905. doi:10.1016/j.fsi.2007.03.004
26. Zhu L, Gu P, Shen H. Gallic acid improved inflammation via NF-κB pathway in TNBS-induced ulcerative colitis. *Int Immunopharmacol*. 2019;67:129–137. doi:10.1016/j.intimp.2018.11.049
27. Reddy DB, Reddanna P. Chebulagic acid (CA) attenuates LPS-induced inflammation by suppressing NF-κB and MAPK activation in RAW 264.7 macrophages. *Biochem Biophys Res Commun*. 2009;381(1):112–117. doi:10.1016/j.bbrc.2009.02.022
28. Zhang H, Wang J, Lang W, et al. Albiflorin ameliorates inflammation and oxidative stress by regulating the NF-κB/NLRP3 pathway in Methotrexate-induced enteritis. *Int Immunopharmacol*. 2022;109:108824. doi:10.1016/j.intimp.2022.108824
29. Diklić M, Mitrović-Ajtić O, Subotički T, et al. IL6 inhibition of inflammatory S100A8/9 proteins is NF-κB mediated in essential thrombocythemia. *Cell Biochem Funct*. 2020;38(4):362–372. doi:10.1002/cbf.3482
30. Wang R, Wang Y, Wu J, et al. Resveratrol targets AKT1 to inhibit inflammasome activation in cardiomyocytes under acute sympathetic stress. *Front Pharmacol*. 2022;13:818127. doi:10.3389/fphar.2022.818127
31. Vickman RE, Aaron-Brooks L, Zhang R, et al. TNF is a potential therapeutic target to suppress prostatic inflammation and hyperplasia in autoimmune disease. *Nat Commun*. 2022;13(1):2133. doi:10.1038/s41467-022-29719-1

32. Rayego-Mateos S, Rodrigues-Diez R, Morgado-Pascual JL, et al. Role of Epidermal Growth Factor Receptor (EGFR) and its ligands in kidney inflammation and damage. *Mediators Inflammation*. 2018;2018:1–22. doi:10.1155/2018/8739473
33. Aihaiti Y, Song Cai Y, Tuerhong X, et al. Therapeutic effects of naringin in rheumatoid arthritis: network pharmacology and experimental validation. *Front Pharmacol*. 2021;12:672054. doi:10.3389/fphar.2021.672054
34. Vogler M. BCL2A1: the underdog in the BCL2 family. *Cell Death Differ*. 2012;19(1):67–74. doi:10.1038/cdd.2011.158
35. Shua Y, Yang N, Bei Y, et al. P-367-PPARγ phosphorylation at Ser186 regulates metabolic inflammation via modulating redox balance in adipocyte tissue macrophages. *Free Radic Biol Med*. 2018;120:S156. doi:10.1016/j.freeradbiomed.2018.04.514
36. Huang LO, Rauch A, Mazzaferro E, et al. Genome-wide discovery of genetic loci that uncouple excess adiposity from its comorbidities. *Nat Metab*. 2021;3(2):228–243. doi:10.1038/s42255-021-00346-2
37. Li Q, Yang Z. Expression of phospho-ERK1/2 and PI3-K in benign and malignant gallbladder lesions and its clinical and pathological correlations. *J Exp Clin Cancer Res*. 2009;28(1):65. doi:10.1186/1756-9966-28-65
38. Koyasu S. The role of PI3K in immune cells. *Nat Immunol*. 2003;4(4):313–319. doi:10.1038/ni0403-313
39. Calissi G, Lam EWF, Link W. Therapeutic strategies targeting FOXO transcription factors. *Nat Rev Drug Discov*. 2021;20(1):21–38. doi:10.1038/s41573-020-0088-2
40. Eijkelenboom A, Burgering BMT. FOXOs: signalling integrators for homeostasis maintenance. *Nat Rev mol Cell Biol*. 2013;14(2):83–97. doi:10.1038/nrm3507
41. Wu J, Huang H, Chen G, et al. Integration of network pharmacology, bioinformatics and experimental verification strategy to discover the pharmacological mechanisms of mogroside acts against pharyngitis. *J Ethnopharmacol*. 2025;344:119499. doi:10.1016/j.jep.2025.119499
42. Dong H, Ying W, Zhu S. Scutellarein ameliorates inflammation and oxidative stress in L-arginine induced acute pancreatitis in mice through regulating the expression of VEGF. *Mol Cell Toxicol*. 2024;20(4):841–849. doi:10.1007/s13273-023-00390-x
43. Olsson AK, Dimberg A, Kreuger J, et al. VEGF receptor signalling -in control of vascular function. *Nat Rev mol Cell Biol*. 2006;7(5):359–371. doi:10.1038/nrm1911
44. Acosta-Martinez M, Cabail MZ. The PI3K/Akt pathway in meta-inflammation. *IJMS*. 2022;23(23):15330. doi:10.3390/ijms232315330
45. Zhang M, Zhang X. The role of PI3K/AKT/FOXO signaling in psoriasis. *Arch Dermatol Res*. 2019;311(2):83–91. doi:10.1007/s00403-018-1879-8
46. Dejean AS, Hedrick SM, Kerdiles YM. Highly specialized role of forkhead box o transcription factors in the immune system. *Antioxid Redox Signaling*. 2011;14(4):663–674. doi:10.1089/ars.2010.3414
47. Graves DT, Milovanova TN. Mucosal Immunity and the FOXO1 Transcription Factors. *Front Immunol*. 2019;10:2530. doi:10.3389/fimmu.2019.02530
48. Yang Y, Sun Y, Hu R, et al. Morphine promotes microglial activation by upregulating the EGFR/ERK signaling pathway. *PLoS One*. 2021;16(9):e0256870. doi:10.1371/journal.pone.0256870
49. Li W, Fang QL, Zhong P, et al. EGFR inhibition blocks palmitic acid-induced inflammation in cardiomyocytes and prevents hyperlipidemia-induced cardiac injury in mice. *Sci Rep*. 2016;6:24580. doi:10.1038/srep24580
50. Wang X, Yu YY, Lieu S, et al. MMP9 regulates the cellular response to inflammation after skeletal injury. *Bone*. 2013;52(1):111–119. doi:10.1016/j.bone.2012.09.018
51. Li Z, Fan Q, Chen M, et al. The interaction between polyphyllin I and SQLE protein induces hepatotoxicity through SREBP-2/HMGCR/SQLE/LSS pathway. *J Pharm Anal*. 2023;13(1):39–54. doi:10.1016/j.jpha.2022.11.005